Consistency properties of chaotic systems driven by time-delayed feedback

T. Jüngling,[*] M. C. Soriano, N. Oliver,[†] X. Porte,[‡] and I. Fischer
Instituto de Física Interdisciplinar y Sistemas Complejos, IFISC (CSIC-UIB), Campus Universitat Illes Balears, 07122 Palma de Mallorca, Spain

(Received 18 July 2017; revised manuscript received 23 March 2018; published 5 April 2018)

Consistency refers to the property of an externally driven dynamical system to respond in similar ways to similar inputs. In a delay system, the delayed feedback can be considered as an external drive to the undelayed subsystem. We analyze the degree of consistency in a generic chaotic system with delayed feedback by means of the auxiliary system approach. In this scheme an identical copy of the nonlinear node is driven by exactly the same signal as the original, allowing us to verify complete consistency via complete synchronization. In the past, the phenomenon of synchronization in delay-coupled chaotic systems has been widely studied using correlation functions. Here, we analytically derive relationships between characteristic signatures of the correlation functions in such systems and unequivocally relate them to the degree of consistency. The analytical framework is illustrated and supported by numerical calculations of the logistic map with delayed feedback for different replica configurations. We further apply the formalism to time series from an experiment based on a semiconductor laser with a double fiber-optical feedback loop. The experiment constitutes a high-quality replica scheme for studying consistency of the delay-driven laser and confirms the general theoretical results.

DOI: 10.1103/PhysRevE.97.042202

I. INTRODUCTION

Synchronization phenomena in networks of dynamical systems have been studied abundantly for three decades [1,2]. Within this paradigm, generalized synchronization has received comparably little attention despite its broad relevance, mostly because of the inherent intricacy of the concept [3–6]. The extension of generalized synchronization to an open environment, in which nonlinear units respond to arbitrary driving signals, has been hardly addressed at all on a fundamental level. In the context of neuroscience, the question about the relationship between external stimuli and the corresponding response of a network of excitable elements is a key to the functionality of the nervous system. In information technology and computer science, networks of nonlinear dynamical systems have been receiving increasing attention with regard to their information-processing capabilities [7,8]. In particular, driven physical systems that naturally support fast nonlinear dynamics are of interest, since they can ideally serve as a hardware basis for fast and efficient implementation of machine-learning schemes [9,10]. With the emergence of complexity science, the network representation of many real-world systems, ranging from the social to the geological domain, offers a new perspective in which the dynamical relationship of local communities to their environmental drive becomes a crucial aspect of investigation [11,12]. In this work, we provide a contribution to the understanding of nonlinear dynamical response beyond conventional synchronization. Our approach follows the idea in Ref. [13], in which the reliability of the signal transformation by a dynamical system is quantified. We focus on the elementary case of a chaotic delay system, where drive and response are identical except for a time shift. This allows us to access analytical relationships that reveal new aspects of delay dynamics, but also have general implications for arbitrary driven systems.

Chaotic dynamics with its irregular and sensitive behavior is a well-known feature of many nonlinear systems. In an externally modulated system, it is not straightforward to identify chaos if the driving signal is irregular, like in the case of information-carrying signals. Certain features of the observed chaos might be a consequence of the drive only, meanwhile others truly originate from instabilities of the driven system [14]. The difference between these cases is that in the former the output is a function of the input, whereas in the latter the dynamical system adds new information. This dilemma has previously been discussed in the context of generalized synchronization, in which the driving signal typically stems from another dynamical system [15,16]. In this regard, there exist a few measures like the conditional Lyapunov exponent (conditional LE or also sub-LE, see Refs. [17–20]) or the degree of consistency [21–23] that can be helpful to clarify which part of the nonlinear response corresponds to the inherent chaotic dynamics and which to the drive.

Consistency refers to the overall degree of intertrial variability produced by the externally modulated dynamical node. A low degree of variability corresponds to a consistent response. In turn, we speak of inconsistency when the distribution of the response states is not significantly affected by the drive, like for instance in case of a small parametric modulation of a

[*]Present Address: School of Mathematics and Statistics, The University of Western Australia, 35 Stirling Highway, Crawley, WA 6009, Australia.
[†]Present Address: Institut für Angewandte Physik, University of Münster, Corrensstraße 2/4, 48149, Münster, Germany.
[‡]Present Address: Institut für Festkörperphysik, Technische Universität Berlin, Hardenbergstraße 36, 10623 Berlin, Germany.

chaotic system. Note that an inconsistent behavior might be unexpected in certain frameworks, although from the perspective of nonlinear dynamics it is a common phenomenon. The level of consistency can be determined by repeating the input signals and comparing the corresponding outputs, for instance via a correlation coefficient [21,24]. Although consistency can only be determined by repetition of driving signals, it is inherent to the nonlinear transformation of signals from input to output, even when not repeatedly driven. Consistency depends on both the properties of the dynamical node and on the driving signals [21]. In the framework of information processing, a consistent response is desired, since inconsistency leads to a certain level of response variation in a task and hence to potentially unreliable computation [25,26]. In contrast to a (sub-)Lyapunov exponent, the consistency correlation is a robust measure that is easier to apply to experimental data. Both measures are not necessarily linked to each other or to the richness of the nonlinear response characteristics that is desired for certain processing tasks. A thorough understanding of the consistency property will be useful to exploit the full range of dynamical responses that a nonlinear node can exhibit.

In this work, we study the consistency correlation of generic chaotic systems driven by time-delayed feedback. Such systems typically have a delay signature in the auto-correlation function (correlation echo or delay echo), which reflects the linear part of the input-output transformation. In contrast to the consistency property, delay echoes can be analyzed sufficiently well from time series of a single system. Delay signatures have been related to strong and weak chaos [27,28]; however, their role within a consistency theory has not been elaborated yet. Our goal is to derive an explicit fundamental relationship between consistency properties and the delay echoes. We achieve this by incorporating in the calculations the correlation echo from the time series of the replica, meaning the response to the repetition of the time-delayed input of the dynamical node. In Sec. II, we introduce the basic theoretical scheme consisting of two delay systems, as well as an extension with functional maps, in which the first forms a closed loop and the second (replica system) forms an open loop driven by the first one. Based on the definition of the correlation functions in this scheme, we split the partially consistent output into a fully consistent component and a fully inconsistent component. By this ansatz, we derive relationships between the correlation measures in the form of outer limits, where a section for a constant level of consistency forms an elliptic domain of allowed correlation values. In Sec. III, we present numerical results for the logistic map with delayed feedback in the consistency scheme, and we compare the correlation functions with the limits given by the ellipse. Further, we extend the scheme to an ensemble of driven maps which allows us to calculate its mean and thus provides support and illustration of the analytical tools of the previous section. In Sec. IV we apply the theoretical framework to time series from a semiconductor laser experiment, validating the theory and providing an understanding of the general results.

II. ANALYTICAL FRAMEWORK

The framework of this study is given by delay systems in the limit of large delays. The response properties of the dynamical node to its own time-delayed feedback can be studied by means of replica setups [4,27,29–34]. In Sec. IV, we report on an experimental realization of such a setup using a semiconductor laser with optical feedback. Here, we aim for a theoretical description of the dynamics in such a scheme in general, which reveals basic relationships between characteristic correlation signatures of delay systems. We will explore these relationships by analyzing the mapping of consecutive time series segments over each delay cycle.

The initial point of our considerations is given by a delay system (closed-loop system) and a copy of the dynamical node driven by the same feedback signal (open-loop system), as described in, e.g., Refs. [34–36] (see also the scheme in Fig. 2),

$$\begin{aligned}\dot{\mathbf{x}}(t) &= \mathbf{f}(\mathbf{x}(t)) + \mathbf{h}(\mathbf{x}(t-\tau))\\ \dot{\mathbf{y}}(t) &= \mathbf{f}(\mathbf{y}(t)) + \mathbf{h}(\mathbf{x}(t-\tau)),\end{aligned} \tag{1}$$

with $\mathbf{x},\mathbf{y} \in \mathbb{R}^N$ and the delay time $\tau > 0$. $\mathbf{f}(\cdot)$ and $\mathbf{h}(\cdot)$ describe the nonlinear response function of the undelayed node and the delayed feedback, respectively. We assume that the delay time is much larger than any characteristic time of the undelayed system, and the trajectories have settled on a—typically chaotic—attractor. Moreover, we consider scalar recordings from the vectorial states as $x(t) = g(\mathbf{x}(t))$ and $y(t) = g(\mathbf{y}(t))$. To simplify matters, let the time series be normalized such that $\langle x(t)\rangle_t = \langle y(t)\rangle_t = 0$ and $\langle x^2(t)\rangle_t = \langle y^2(t)\rangle_t = 1$, with the average denoting $\langle x(t)\rangle_t = \lim_{T\to\infty} \frac{1}{T}\int_0^T dt\, x(t)$. These infinite stationary time series are then split into consecutive delay intervals such that $x_n(t) = x(t+n\tau)$ and $y_n(t) = y(t+n\tau)$ with $t \in [0,\tau[$ and $n \in \mathbb{N}$. With the extra discrete time index n, the set of segments can be understood as the "spatiotemporal" representation of the delay systems [37]. We are interested in the mapping of one τ-segment to the next. One might formally consider a functional map of the form $\mathbf{x}_{n+1} = \mathcal{G}(\mathbf{x}_n)$ that follows from Eq. (1). Such a deterministic rule applies only to the vectorial states and not to the scalar projections. The main problem, however, is the inappropriate representation of the evolution of different initial conditions, that gives rise to the difference in x and y. The same argument holds for the reaction to a small amount of intrinsic noise as it appears in experimental realizations of delay systems. We therefore consider a different model that acts as an extension to the above delay systems. The evolution of τ-segments $x_n(t)$ and $y_n(t)$ will be governed by stochastic maps:

$$\begin{aligned}x_{n+1} &= \mathcal{F}(x_n) + \xi_n,\\ y_{n+1} &= \mathcal{F}(x_n) + \eta_n.\end{aligned} \tag{2}$$

Here, $\mathcal{F}(\cdot)$ represents a nonlinear functional map acting on the time series of length τ. The additional signals $\xi_n(t), \eta_n(t)$ are independent realizations of a noise process with limited variance and correlation time. The introduction of the noise terms is motivated by three arguments. First, as compared to the deterministic Eq. (1), the noise accounts for the loss of information about the vector state in the scalar signals. Second, a delay system can exhibit strong chaos, meaning that the nonlinear node's response to the drive exhibits an instability at a timescale much shorter than the delay time. This instability amplifies different initial conditions and small intrinsic

noise, resulting in different responses despite receiving the same drive. The noise terms account for this type of chaotic variability. Third, both intrinsic noise and measurement noise, directly contributes to ξ and η. The main difference between both models lies in the (non-)existence of a synchronous solution $x(t) = y(t)$, regardless of its stability. It exists for the noise-free delay systems, but not for the stochastic map, unless further constraints are applied to the noise terms. The theory that we develop in the following holds for time series obtained from both models. We will use an explicit example of the delay systems in Sec. III.

The causal structure given by Eqs. (1) and (2) typically leaves measurable relationships in the resulting time series. In this work, we restrict our analysis to linear correlation functions. On the one hand, their explanatory power might be limited—in particular for nonlinear systems—although their main advantage is their fast calculation and their straightforward interpretation. On the other hand, a sophisticated nonlinear relationship is mapped to a simple linear correlation by virtue of the replica setup, thus extending its relevance beyond conventional linear relationships. Apart from the replica scheme, a recent work also demonstrated how details of the correlation function can contain valuable fingerprints of dynamical features of the system, despite its apparent simplicity [38]. Figure 1 shows an example of autocorrelation (AC) and cross-correlation (CC) functions obtained from time series of a replica setup with the logistic map with delay according to Eq. (19).

While the general shape of such correlation functions might deviate significantly from the depicted example, a common feature among many nonlinear delay systems is the occurrence of a delay echo. The delay signature or delay echo is a peak structure in the AC and CC functions characterized firstly by a certain height and width; see Figs. 1(d)–1(f). The aforementioned criterion of timescale separation between delay time and the timescale of the oscillator can be expressed by a clear separation of the different peak structures or by the delay time being much larger than the characteristic width of the delay echo. It was shown that, in this large delay regime, the shape of the delay echoes does not change under a variation of the delay time, while the position of the peak relative to the delay time is fixed [28]. In the following, we focus on selected values of the correlation functions within the peak structures. These can be either the largest peak, regardless of its sign, or the correlation at integer multiples of the delay time, considering also a small and arbitrary offset from the delay time as long as it remains within the peak structure. In the example shown in Fig. 1, the position of the peak coincides with the delay time, however, this is not generally the case as can be seen in the examples in Fig. 6; see also Ref. [38]. For the sake of simplicity, we will refer to the selected correlations as "peaks" and specify the corresponding time shift for detailed analysis.

There are two fundamentally different contributions behind each of the peaks. First, a correlation peak might reflect a causal relationship. In our scheme, the first echoes of AC and CC (peaks labeled "α" in Fig. 1) correspond to the underlying direct connection. This means that the external signal, here from the delay term $\mathbf{x}(t-\tau)$, is injected in both systems and thus causally affects $\mathbf{x}(t)$ and $\mathbf{y}(t)$ in the same way; see also Ref. [39]. Second, a peak might indicate the correlation only

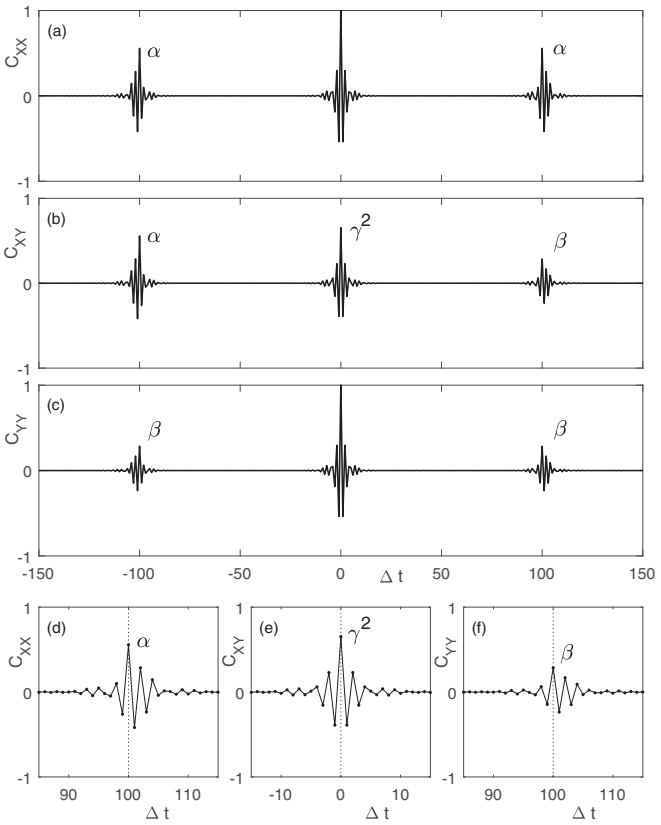

FIG. 1. Correlation functions from time series of delay-coupled logistic maps, Eq. (19) for $k = 0.3$ and $\tau = 100$, showing characteristic peak structures. (a) Autocorrelation function of closed-loop system. (b) Cross-correlation function between closed-loop and open-loop system. (c) auto-correlation function of open-loop system. (d)–(f) Zoom into the peak structures from (a)–(c), respectively. In this example, delay time and peak position coincide.

because of a corresponding correlation in the drive. The central peak of the CC (peak "γ^2") stems from the identical drive and cannot arise from an instantaneous communication between the systems. The same argument holds for the first AC echo in the replica system which compares $y(t-\tau)$ with $y(t)$ (peak "β"). Since the replica has no feedback, this peak only reflects the underlying correlation between $x(t-\tau)$ and $x(t)$. Memory from the dynamical unit causing this echo is excluded, as it is closely related to the width of the peak structures, whereas the echo is linked to the delay time. It is worth mentioning that, apart from these causal relationships, the γ^2 peak also plays a distinct role because of its connection to the complete synchronization manifold $x(t) = y(t)$ in the noise-free Eq. (1). The peak indicates the closeness of the trajectories to the completely synchronous solution. In contrast, there are no trivial manifolds related to the α and β peaks, regardless of which time shift within the corresponding echoes is considered.

The goal of this work is to derive general relationships between the different correlation peaks, based on the replica scheme, on consistency properties, and on the interplay of the aforementioned principles related to causality. To this end, we structure the dynamics generating the time series $x(t)$ and $y(t)$ in a way as indicated symbolically in Fig. 2. We define

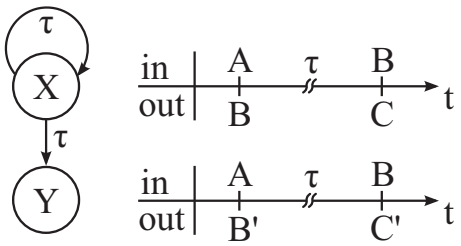

FIG. 2. Basic structure for the analytics. Left: Coupling scheme corresponding to the auxiliary system approach. Right: Symbolic representation of input and output for time series from X and Y.

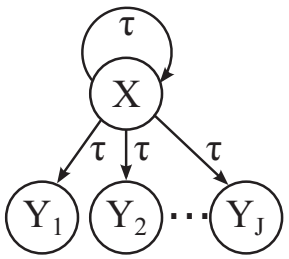

FIG. 3. Illustration of an ensemble of J replica systems attached to a single closed-loop unit.

four pairs of input and output vectors, (A,B), (B,C), (A,B'), and (B,C'). Each vector corresponds to a τ-segment $x_n(t)$ or $y_n(t)$ for different consecutive iterations n of either the space-time representation of Eq. (1), or directly from the more general Eq. (2). In this manner, we have defined a rename and duplication procedure towards a new set of time series. These time series take into account the structure given by the replica scheme, in which $x(t-\tau)$ is a component of the common input underlying $x(t)$ and $y(t)$. The original idea for this trivial but helpful step is motivated by the iterative generation of τ-segments in the delay system by passing of the signals through the nonlinear node [37,39–41]. Although we allow the limit $\tau \to \infty$ as well, we introduce overlaps for finite τ by extending the vectors to the entire time series instead of the τ-segment. With this procedure we do not deteriorate any feature based on the original idea while gaining the possibility to average over long time. In detail, we set $A(t) = x(t-\tau)$, $B(t) = x(t)$, and $C(t) = x(t+\tau)$, and analogously $B'(t) = y(t)$ and $C'(t) = y(t+\tau)$. Such assignments could be extended to include further multiples of the delay time, but considering the shown four drive-response pairs turns out to be sufficient to derive the basic relationships of the correlation echoes. A possible extension is given by changing the time shift from τ to $\tau + \delta$, where δ is chosen to point at the peak position or an arbitrary position within the delay echoes. The same relationships are expected to hold when such a small 'reaction time' related to the inertia of the dynamical system is included as a part of the signal transformation, so that a time shift equal to τ can be considered without loss of generality.

A. Correlation measures

We start by defining the *transformation correlation* as the linear relationship between input and output in terms of the above vectors. The term *transformation* gives credit to the fact that an input waveform passes through a dynamical (nonlinear) node that generates an output waveform. With the normalization of the time series as introduced above, four pairs satisfy the equality

$$\langle AB\rangle = \langle BC\rangle = \langle AB'\rangle = \langle BC'\rangle = \alpha, \tag{3}$$

where the averages are taken over time t. The equality can first be explained by time-translation symmetry for each system. Second, all vectors have the same statistical properties because of stationarity. We assume ergodicity in the sense that the output of the original and of the replica system are equivalent realizations of the same process, yielding identical time averages. The first and the second term are the AC coefficient $\langle x(t)x(t+\tau)\rangle$, whereas the third and the fourth are the CC coefficient $\langle x(t)y(t+\tau)\rangle$. From the time shift we see that this refers to the first delay echo.

We are further interested in the cross-correlation without time shift $\langle x(t)y(t)\rangle$, which relates to the identical synchronization manifold. This is the *consistency correlation* [23], and it reads

$$\langle BB'\rangle = \langle CC'\rangle = \gamma^2. \tag{4}$$

The final correlation measure is the first delay echo of the response system, $\langle y(t)y(t+\tau)\rangle$, which is the *spurious correlation*

$$\langle B'C'\rangle = \beta. \tag{5}$$

Notably, the same echo appears in the cross-correlation function $\langle y(t)x(t+\tau)\rangle$; see Fig. 1. This identity is less clear than the match of the α-echoes, unless further insight into the consistency properties is provided.

B. Consistency properties

For the following steps, we attach $J \gg 1$ replica units $Y_1, \ldots Y_J$ to our setup, such that together with X we have in total $J+1$ identical dynamical systems driven by the same signal; see Fig. 3. Each unit has been initiated with slightly different initial conditions. In the limit $J \to \infty$, their responses $B_1(t), \ldots B_J(t)$ form a distribution $\rho_B(t)$. In the same way, we define the distribution $\rho_C(t)$, which is connected to ρ_B via time translation $\rho_B(t+\tau) = \rho_C(t)$. Using these distribution functions we calculate an ensemble average, which can be interpreted as the consistent component F of the responses B and C; as well as B' and C' of X and Y, respectively,

$$\begin{aligned} F_A(t) &= \langle B_i(t)\rangle_i = \langle B_i'(t)\rangle_i = \int z\rho_B(z,t)dz, \\ F_B(t) &= \langle C_i(t)\rangle_i = \langle C_i'(t)\rangle_i = \int z\rho_C(z,t)dz. \end{aligned} \tag{6}$$

The different notations B_i and B_i' (or C_i, C_i') give credit to the fact that the additional replica units can be understood as an ensemble of possible realisations of the original X or the single replica Y, respectively. The main point here is that both systems have a common mean response. The idea of an ensemble of responses with their mean reflecting a very general form of synchronization to the drive is essentially different from the conventional forms of synchronization and has been

elaborated on in Ref. [13]. In Appendix 1 we show how our ansatz can be interpreted as being specifically motivated by the correlation coefficients which we apply to the time series. In other words, the consistent component of the response depends on the measure characterizing the conditional density of the response system. In our case, the inconsistent component N follows consequently as the difference between consistent component and the original vector:

$$\begin{aligned} F_A(t) + N_A(t) &= B(t), \\ F_B(t) + N_B(t) &= C(t). \end{aligned} \tag{7}$$

The indices indicate that the signals result from a response from the inputs A and B, where F suggests the presence of a functional relationship and N the modeling of a noiselike process, like in Eq. (2). In this picture, by definition it follows that

$$\begin{aligned} F_A(t) + N'_A(t) &= B'(t), \\ F_B(t) + N'_B(t) &= C'(t), \end{aligned} \tag{8}$$

meaning that the consistent components of the responses agree in both realizations, whereas the inconsistent components are different. One can further calculate the properties of the time averages:

$$\langle F_A \rangle = \langle F_B \rangle = \langle N_A \rangle = \langle N'_A \rangle = \langle N_B \rangle = \langle N'_B \rangle = 0.$$

Less trivial is the property of the consistent and inconsistent components not to be correlated, neither the inconsistent components among each other, see Appendix 2,

$$\langle F_A N_A \rangle = \langle F_A N'_A \rangle = \ldots = 0, \tag{9}$$

$$\langle N_A N'_A \rangle = \langle N_A N_B \rangle = \ldots = 0. \tag{10}$$

The timescale separation due to the large delay is an important precondition for this feature. However, there is one important exception. In contrast to the independent signal N'_A from the response system, the signal N_A from the drive system is underlying the generation of the signal C, which implies a nonzero correlation:

$$\langle F_B N_A \rangle \neq 0. \tag{11}$$

This term highlights the main difference between closed loop and open loop. The corresponding counterpart $\langle F_B N'_A \rangle$ is zero, because N'_A does not causally affect F_B.

We use the decomposition in consistent and inconsistent component to express the correlation measures Eqs. (3)–(5). For the consistency correlation we obtain

$$\begin{aligned} \langle BB' \rangle &= \langle (F_A + N_A)(F_A + N'_A) \rangle \\ &= \langle F_A^2 \rangle \\ &= \gamma^2. \end{aligned} \tag{12}$$

In terms of the presented decomposition of the vectors, we can also write the expression for the AC echoes (transformation correlation)

$$\begin{aligned} \langle BC \rangle &= \langle (F_A + N_A)(F_B + N_B) \rangle \\ &= \langle F_A F_B \rangle + \langle N_A F_B \rangle \\ &= \alpha. \end{aligned} \tag{13}$$

Here we see the transfer of information due to the self-feedback in the second term. In contrast, in the AC echo of the response system (spurious correlation) this term is missing

$$\begin{aligned} \langle B'C' \rangle &= \langle (F_A + N'_A)(F_B + N'_B) \rangle \\ &= \langle F_A F_B \rangle \\ &= \beta. \end{aligned} \tag{14}$$

The identity of the AC and the CC echoes can also be shown using the properties of the consistent and inconsistent components in Eqs. (9)–(11). Changing the ansatz in Eq. (13) yields $\langle BC' \rangle = \alpha$, and accordingly the counterpiece of Eq. (14) is $\langle B'C \rangle = \beta$.

C. Estimation of the correlation echoes

Due to time translation symmetry, the size of the vectors F_A and F_B is both γ. The desired correlation measure, $\beta = \langle F_A F_B \rangle$, is therefore determined by the angle between them. Trivially, we can already conclude that the product will be bounded by

$$|\beta| \leqslant \gamma^2.$$

Using information from the transformation correlations we can derive a stronger estimate. We know from the principal identity of these correlations that we obtain α also from the projection of B and C', where the inconsistent component of C' drops

$$\alpha = \langle BC' \rangle = \langle BF_B \rangle.$$

Since B is a unit vector and the size of F_B is γ, we can write for the angle φ between them

$$\cos\varphi = \frac{\alpha}{\gamma}.$$

Second, we can use the decomposition of B into its own consistent and inconsistent component to calculate the angle θ between B and F_A,

$$\cos\theta = \gamma.$$

We cannot specify further the orientation of B, F_A, F_B in their three-dimensional subspace, which leads to the restriction of the angle between F_A, F_B. The final expression for the upper and lower bounds for β reads

$$\begin{aligned} \beta_\pm &= \gamma^2 \cos\left(\arccos\frac{\alpha}{\gamma} \pm \arccos\gamma \right) \\ &= \gamma^2 \left[\alpha \pm \sqrt{(1-\gamma^2)\left(1 - \frac{\alpha^2}{\gamma^2}\right)} \right]. \end{aligned} \tag{15}$$

This defines an ellipse in the space of α, β as shown in Fig. 4. The extension of the ellipse on the parameter axes implies a relationship between transformation correlation and consistency correlation,

$$|\alpha| \leqslant \gamma. \tag{16}$$

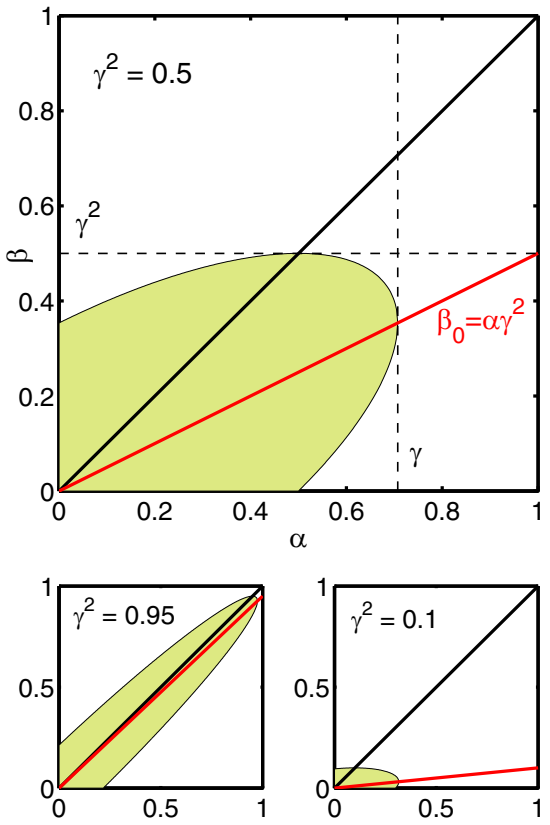

FIG. 4. Graphical illustration of the relationships between α and β given a fixed value of $\gamma^2 = 0.5$ (top), $\gamma^2 = 0.95$ (bottom left), and $\gamma^2 = 0.1$ (bottom right). Black solid line: identity $\alpha = \beta$. Red (gray) solid line: neutral line $\beta_0 = \alpha\gamma^2$. Shaded region: generally allowed relationships according to consistency theory. The intersections of the ellipse with the linear functions are at its outmost extensions with tangents $\alpha = \gamma$ and $\beta = \gamma^2$ (black dashed lines in top panel).

Together with the bound $|\beta| < \gamma^2$, this relation shows how the consistency property fundamentally affects the correlation echoes.

Within the elliptic domain formed by the consistency boundaries, there is no *a priori* preference for the location of correlation pairs (α,β), unless system-specific information is included. Nevertheless, a distinct constellation is given by the case when the plane spanned by B, F_B is perpendicular to the plane of B, F_A. The interpretation of this geometry is that the consistent component of the output (here F_B) has no preference between the consistent (F_A) or the inconsistent component (N_A) of the input. This argument defines the mean of β_+ and β_-, which is

$$\beta_0 = \alpha\gamma^2. \tag{17}$$

Figure 4 illustrates the analytical boundaries including this "neutral line" for different values of the consistency correlation γ^2.

The meaning of γ, in addition to the interpretation of γ^2 as the consistency correlation, becomes clear by treating the consistent component of the responses as an independent signal. In contrast to Eq. (12), in which the magnitude of F_A was preserved, we apply here the normalization as for the time series from individual units. With $\tilde{F}_A = F_A/\sqrt{\langle F_A^2\rangle} = F_A/\gamma$ we obtain the correlation

$$\begin{aligned}\langle B\tilde{F}_A\rangle &= \langle (F_A + N_A)F_A/\gamma\rangle \\ &= \langle F_A^2\rangle/\gamma \\ &= \gamma. \end{aligned} \tag{18}$$

The consistent component yields the optimal prediction of the output state of the driven nonlinear system given only the input. Optimality is understood in the sense of a least-squares fit given the ensemble of all possible responses, which is equivalent to the ensemble mean and maximizes the correlation. Thus, the coefficient γ is the degree of complete consistency which is inherent to the signal transformation. It defines the limit of predictability without inclusion of the initial conditions of the driven system, which in turn affects the information transfer through the system. The reduced value of $\gamma^2 \leqslant \gamma$ is a consequence of the inconsistent component N'_A of a single replica unit that deteriorates its relationship to the original system as compared to the mean of many replicas. In Fig. 5 we demonstrate this principle by the excellent agreement of the value of $\sqrt{\gamma^2}$ from the single replica with γ from an ensemble mean according to Sec. III B.

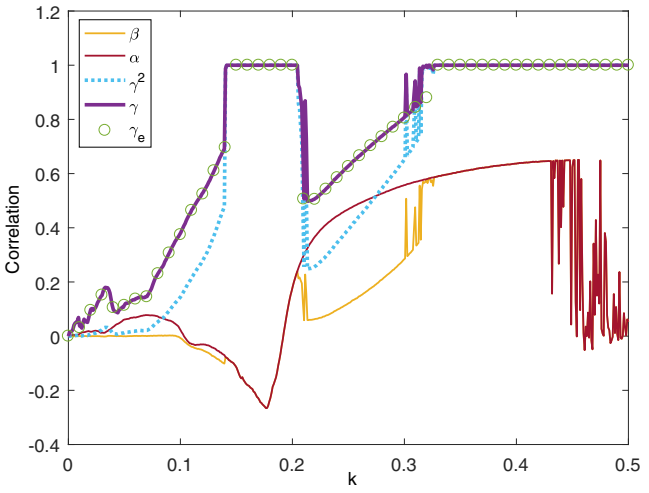

FIG. 5. Correlations of logistic map with feedback Eq. (19); see text. α and β are the values of the autocorrelation functions of x and y, respectively, taken at time shift $\Delta t = \tau = 30$. The consistency correlation γ^2 and its root are plotted to validate the outer extensions of the ellipse on the α- and β-axis. The additional γ_e (circles) is the correlation between x and the ensemble mean of replicas [using Eqs. (20)–(21) with $J = 1000$ and Eq. (18)], which coincides with $\sqrt{\gamma^2}$ from a single replica.

III. EXAMPLE: LOGISTIC MAP WITH DELAYED FEEDBACK

In the following, we exemplarily study the logistic map with delayed feedback numerically, which is discrete in time and has an explicit nonlinearity in its feedback and instantaneous term [42]. We consider two cases. First, a single replica unit is attached to the delayed map, and the correlation signatures of this auxiliary system set are calculated and compared to the

general framework. Second, we attach a set of many replica forming an ensemble, from which we are able to determine the consistent and inconsistent component of the responses, and thus illustrate and test the analytical calculations of Sec. II.

A. Two maps in the auxiliary system setup

The replica setup for the delayed discrete map reads

$$\begin{aligned} x_{t+1} &= (1-k)M(x_t) + kM(x_{t-\tau}), \\ y_{t+1} &= (1-k)M(y_t) + kM(x_{t-\tau}), \end{aligned} \tag{19}$$

with $M(x) = 4x(1-x)$ revealing the logistic map for $k = 0$. For the analysis, the default normalization of the time series x_t and y_t are applied. For $k \in [0,0.5]$ and $\tau = 30$, the basic correlation signatures are depicted in Fig. 5, where α and β are picked up at time shift $\Delta t = \tau$, and both ellipse edges γ and γ^2 are plotted. Indeed, the relations $|\alpha| < \gamma$ and $|\beta| < \gamma^2$ are fulfilled over the entire range. The same holds true if α and β were selected to be the peak values whose position does not necessarily coincide with τ at all k (not shown in Fig. 5, see the examples in Fig. 6). We recall that, unlike the flexibility for α and β, the consistency correlation is always calculated from the CC at zero time shift. The map offers a large variety of different correlation triples. Most significant are the phase flip around $k = 0.2$ within the first consistent region, the flat response of β for $k < 0.1$, and the observation that α largely follows a smooth curve whereas β seems to repeat the consistency breakdowns. The latter highlights the subtle intrinsic nature of consistency, which is not directly reflected in the AC echo α, and hence sets the demand for the replica scheme. Moreover, the similarities between the β and γ curve support the neutral line hypothesis: The AC peak α—apart from being bounded by γ—develops largely independently, but the open-loop peak β is explicitly linked to the consistency by $\beta = \alpha\gamma^2$. Consequently, β and γ^2 show the same structures like the sharp breakdowns in the inconsistency episodes. Finally, it is worth mentioning that the disruptive behavior for $k > 0.42$ in the completely consistent regime is related to a change in the dynamics from chaotic to (quasi-)periodic behavior. The central correlation peak and the delay echoes merge to a coherent structure corresponding to the sustained oscillations.

For some selected feedback values, the entire CC function and the peak structures in the corresponding ellipse are shown in Fig. 6. It is sufficient to focus on the CC only, because in the ideal replica setup simulated here the corresponding AC and CC peaks for α and β are identical. We plot the entire peak structure $\alpha(\Delta t)$ and $\beta(\Delta t)$ with a simultaneous time shift $\Delta t = -\tau - \delta$ and $\Delta t = \tau + \delta$, respectively. The offset δ is chosen such that the peak envelope is above a small threshold value. The ellipse boundaries are not violated by the correlations, but the peak values can approach the edge closely. The resulting structures orient along the neutral line (blue dashed line in Fig. 6), and deviations stay small. It is remarkable that the aforementioned sign flip in the echoes comes along with a flip in the preferred side on which the echo structure deviates from the neutral line (compare $k = 0.125$ with $k = 0.25$).

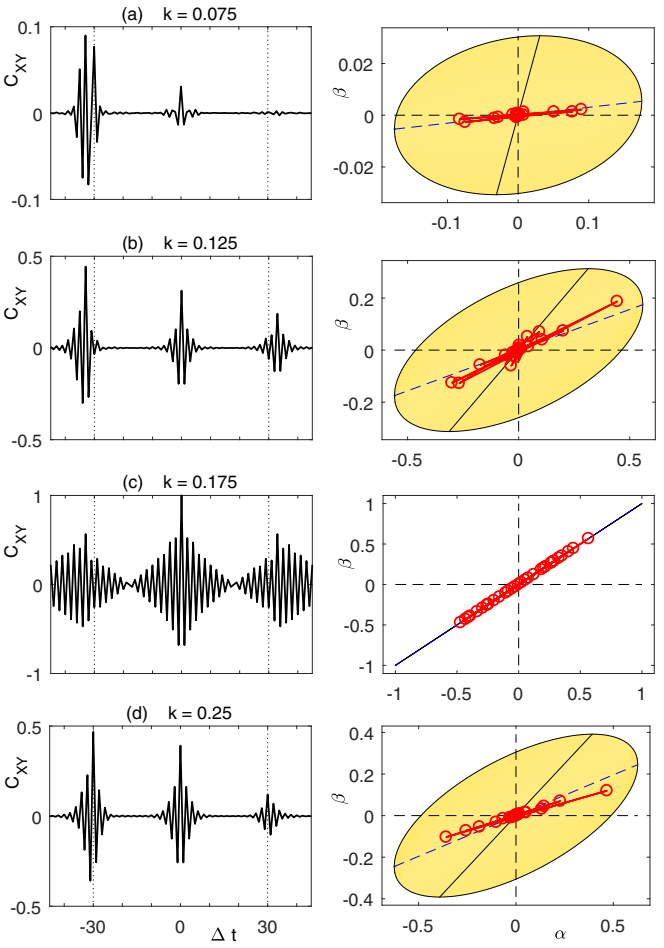

FIG. 6. Examples of correlation parameters from the coupled logistic maps, see Eq. (19), drawn in the corresponding ellipse. Left: entire cross-correlation function between x_t and y_t, including the first delay echoes around the delay time $\tau = 30$. The value at zero time shift corresponds to γ^2 and the vertical extent of the ellipse, α (β) is picked up from the peaks at the negative (positive) time shift. Right: Corresponding ellipses (yellow/light gray) with entire delay echoes plotted inside (red/dark gray) including the neutral line $\beta_0 = \alpha\gamma^2$ (gray, dashed).

B. Ensemble of many identical maps

To illustrate and support the derivations in Sec. II, we calculate numerically an ensemble of discrete maps (see Fig. 3), which allows us to study the consistent and inconsistent components of the trajectories separately. The nonlinear dynamical node contains again the quadratic function $M(x) = 4x(1-x)$ from the logistic map, as in the previous section. Here, we consider a closed-loop delay system $\mathcal{X}$ with J open-loop attached units $\mathcal{Y}_1 \ldots \mathcal{Y}_J$ following the equations

$$\begin{aligned} x_{t+1} &= (1-k)M(x_t) + kM(x_{t-\tau}), \\ y_{1,t+1} &= (1-k)M(y_{1,t}) + kM(x_{t-\tau}), \\ &\vdots \\ y_{J,t+1} &= (1-k)M(y_{J,t}) + kM(x_{t-\tau}). \end{aligned} \tag{20}$$

Normalization of the resulting individual time series is applied as in the previous sections.

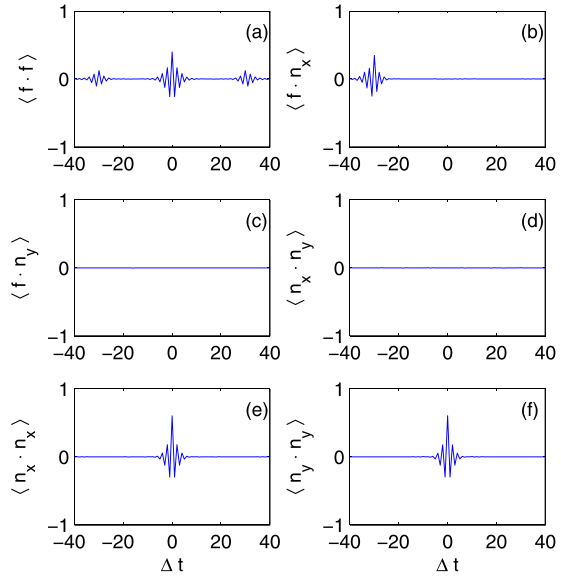

FIG. 7. Pairwise projections of the consistent component f and the inconsistent components n_x,n_y of the responses x and y, obtained from Eq. (20) for delayed logistic maps with delay $\tau = 30$. Time shifts Δt range from -40 to 40 to include τ. (a) Projection of the consistent components. (b) Consistent component f and inconsistent component n_x showing the peak related to the closed-loop connection. (c) No correlation between f and n_y in open loop. (d) No correlation between inconsistent responses n_x and n_y due to independence. (e, f) Autoprojection of n_x and n_y, respectively, identical and without delay echoes.

The ensemble average is calculated as

$$f_t = \frac{1}{J}\sum_{j=1}^{J} y_{j,t}. \tag{21}$$

It corresponds to the consistent component of the responses F_A and F_B from the symbolic representation. Having calculated f_t, we go back to the minimal set of closed-loop x_t and open-loop $y_t \equiv y_{1,t}$. The inconsistent components of these two trajectories are $n_{x,t} = x_t - f_t$ and $n_{y,t} = y_t - f_t$. The former corresponds to the symbolic N_A and N_B and the latter to N'_A and N'_B, respectively, when applying proper time shifts.

We calculate the pairwise scalar products of the vectors f,n_x,n_y with time shifts such that contributions to the correlation functions of x and y are visualized. These pairwise projections are shown in Fig. 7. Parameters of the simulation are $k = 0.25, \tau = 30, J = 10^5$. There are six possible combinations shown in the corresponding panels. In the self-projection of the consistent component f [Fig. 7(a)], the resulting function includes the measure γ^2 in the central peak and β in the symmetric side peaks; see Eqs. (12) and (14). When projecting f onto n_x or n_y [Figs. 7(b) and 7(c)], their independence, except for a single peak, becomes visible; see Eqs. (9) and (11). This peak indicates the closed-loop property of system $\mathcal{X}$ and occurs only at the point where n_x causally affects f. The cross-projection of n_x and n_y [Fig. 7(d)] illustrates the independence of these vectors according to Eq. (10), whereas their autoprojections are identical and reveal the value $1 - \gamma^2$ at zero time shift [Figs. 7(e) and 7(f), respectively]. The delay echoes are eliminated in both, because inconsistency is generated locally regardless of the delay loops. In summary, the result from the map ensemble agrees in all aspects with the analytically derived relations.

IV. SEMICONDUCTOR LASER EXPERIMENT

Semiconductor lasers with fiber-optical feedback provide an excellent testbed for experiments on delay dynamics. We analyze intensity time series of delay-driven chaotic lasers and study their correlation properties in the context of the presented consistency theory. A semiconductor laser subject to delayed optical feedback is known to exhibit instabilities that can result in high-dimensional chaotic behavior [43]. Under the conditions of long delays, the complex optical waveforms generated by the delay system can often be treated as an external drive to the laser. This drive then again excites a dynamical response of the laser. The response exhibits the same statistical properties as the drive, as soon as the delay system has settled on its chaotic attractor. In general, the degree of consistency of the delayed feedback laser response will mainly depend on conditional stability. By means of time series analysis of a single laser with feedback, it is difficult to access this property directly and reliably [20]. Both, the analysis of the sub-LE, as well as the consistency property would benefit from recurrences in the (Banach) state space of the delay system, meaning that highly similar patterns reoccur at different points in time. For the typically large delays, this is very rare, as a reasonably long time series does not sample the huge state space sufficiently. We, therefore, rely on a replica experiment, in which we can capture at least two different laser responses to the same driving signal and compare them directly.

A. Experiment

An elegant realization of a replica scheme is given by an experiment in which a single laser is repeatedly driven with the same optical waveform, generated by itself under delayed feedback conditions. Recording the signal and replaying it repeatedly is difficult for systems with optical feedback. Although feasible for scalar drive signals, this is very challenging for the high-bandwidth signals with amplitude and optical phase, generated by the typical complex chaotic dynamics. Amplitude and optical phase fluctuations are coupled, and the fastest components reach up to tens of GHz in frequency. Therefore, it is required to store the signal by optical means.

A possible manner to realize optical storage and replay is to branch off a part of the light from the primary feedback loop, by which the dynamics is generated, and to transmit it in a much longer second fiber that acts as an optical memory. The double-delay-loop scheme is illustrated in Fig. 8. The semiconductor laser in our experiment is a discrete-mode laser lasing at 1544 μm and exhibiting a threshold current of $I_{\text{th}} = 11.8$ mA without feedback. The laser light is split, and simultaneously enters two optical fiber loops with significantly different propagation delays: $\tau_1 = 111$ ns for the short loop and $\tau_2 = 21$ μs for the long loop. To switch between short and long loop we employ electro-optic modulators controlled by a pulse generator, such that one path is blocked at any time. This experimental scheme has been presented in an earlier work

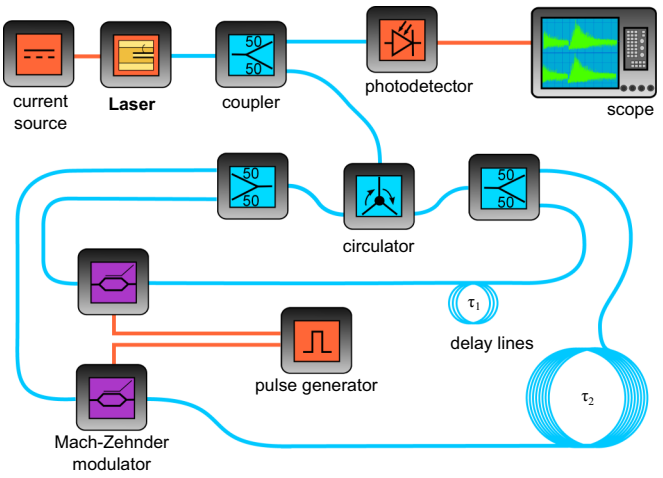

FIG. 8. Simplified scheme of the double-delay-loop experiment. The laser is subject to optical feedback from either a short delay line or a long one. A pulse generator in combination with two Mach-Zehnder modulators controls that only one of the feedback paths at most is active at any given time.

[23]. In the same work, consistency correlation was discussed and compared with the autocorrelation echoes of short and long loop, corresponding to all of the relevant theoretical quantities of the consistency theory, i.e., the peak values γ^2, α, and β. Therein, however, the latter two delay echo peaks were only obtained from the AC, and further information from the peak structures had not been analyzed.

B. Time series and correlation signatures

The intensity time traces of short-loop and long-loop dynamics already reveal the high degree of consistency attainable with the double-delay-loop experiment. The sample shown in Fig. 9 covers a window of 10 ns. The time traces have been deskewed to account for the difference in delay lines so that both responses can be directly compared. As a convention, we will also speak of original and replica to refer to the time-corrected short-loop and long-loop dynamics, respectively. The temporal oscillations match in phase and amplitude most of the time, displaying only small deviations that are quickly recovered. This behavior, corresponding to $I = 1.48 I_{\text{th}}$, is considered a dynamical regime with a high level of consistency. Nevertheless, it is through the calculation of the consistency

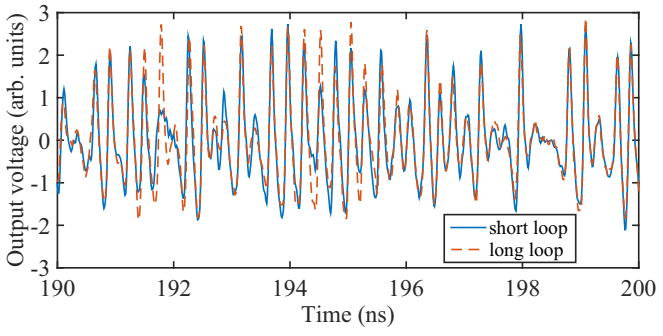

FIG. 9. Temporal dynamics from short and long loop acquired for a pump current of $I = 17.5$ mA. The time traces have been deskewed to overlap in time.

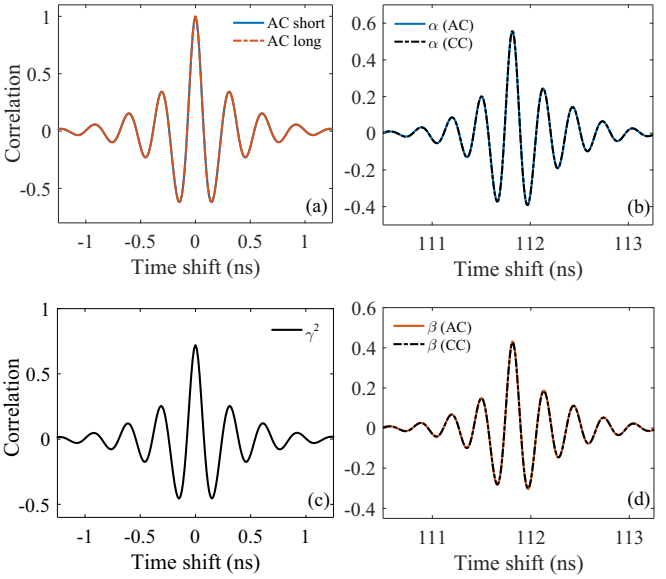

FIG. 10. Correlation peaks in the double-delay-loop experiment. (a) Central peak structure of AC from original and replica coincide. (b) First delay echo α of original AC and CC coincide. (c) Central CC peak structure is symmetric and reveals consistency correlation γ^2 at its center. (d) First delay echo β of replica AC coincides with CC where original and replica is exchanged.

correlation γ^2 that the similarity of the responses can be quantified. The average optical power in the long fiber loop remains relatively low (<0.5 mW) for pump currents below $2I_{\text{th}}$ so that fiber nonlinearities can be excluded.

Beyond the mere extraction of the correlation measures, the study of the entire correlation functions can also elucidate characteristic relationships between the delay echoes. Figure 10(a) shows the central peaks of the AC curves for the original (short loop) and replica (long loop). The perfect agreement of both curves indicates the identical statistical properties of the short-time patterns. The peak structures for the delay echoes of α and β are illustrated in Figs. 10(b) and 10(d), respectively. The correlation peaks for α and β are not symmetric around the center, but still coincide for AC and CC functions. A high degree of proportionality between α and β is also unveiled. Here, the peak structure of α obtained from the CC has been mirrored to a positive time shift to overlay the curve. The oscillations from the central CC peak as shown in Fig. 10(c) contain valuable information related to consistency. The structure is symmetric and a scaled-down version of the AC peaks shown in Fig. 10(a). We discuss the meaning of these signatures further in Sec. IV D.

Figure 11 shows a complete picture of the correlation quantities as a function of the pump current. The consistency correlation γ^2 exhibits a single minimum around 13 mA and increases with the pump current until it saturates in values close to 0.99 [23]. Considering that γ^2 is calculated from the central peak of the cross-correlation function, this degree of consistency reflects the high quality of the replay by the long loop. The transformation correlation α and the spurious correlation β follow largely the same trend as the consistency correlation. The disparity between α and β is intrinsic to the

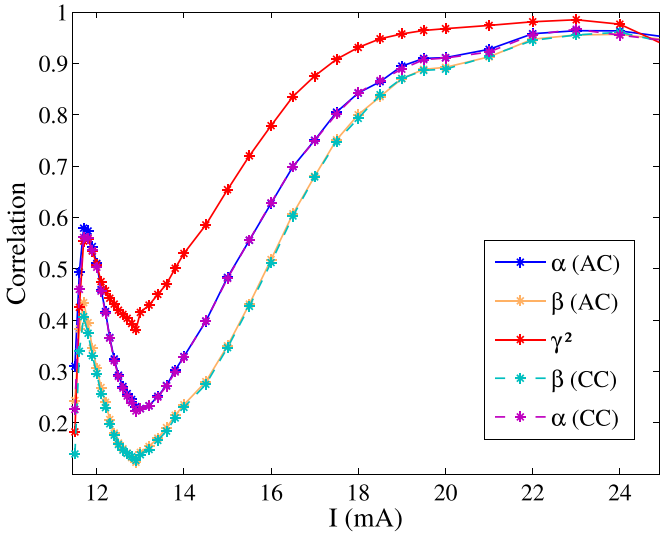

FIG. 11. Five selected peak values of correlation functions in dependence on the pump current I of the laser: Consistency correlation γ^2 from CC, transformation correlation α from AC of original and CC (coinciding), and spurious correlation β from AC of replica and CC (coinciding).

consistency properties and satisfies the theoretical relationships from Sec. II, which we will further discuss in Sec. IV C. Under ideal conditions, the two correlation coefficients can be obtained from the autocorrelation function, as well as from the cross-correlation, where the delay echoes are identical. Remarkably, the experimental data provides the same correlation values within high accuracy, as they perfectly overlap in the plot. Moreover, when we resolve the entire echoes as in Fig. 10, the match between AC and CC signatures is excellent.

C. Delay echoes and the consistency ellipse

The theoretical framework from Sec. II provides a unifying perspective on correlations in delay systems based on the concept of consistency. The key ingredient of this theory is a decomposition of the dynamical response into a completely consistent component and an inconsistent component that leads to basic relationships between the presented correlation measures α, β, and γ^2. They are essentially obtained from the three central peak structures in the cross-correlation function between original and replica time series. In previous works, α had been used as an indicator of the consistency property, and the similarity with the revealed γ^2 values confirms this particular finding for semiconductor lasers with optical feedback [23]. The intuition behind the apparent proportionality between α and γ^2 already leads into the right direction: Inconsistency caused by a positive sub-LE means a high degree of variability in the output given a certain input. When input and output are then directly compared, the correlation coefficient will consequently be limited by the degree of inconsistency. This is quantitatively reflected in the bound $|\alpha| < \gamma$. In the laser experiment the stronger relationship between α and γ is a system-specific property.

To shed more light on that argument we look at a counterexample provided by the Ikeda delay system $dx(t)/dt = -x(t) + \kappa \sin[x(t-\tau)]$. This system is completely consistent because of the sub-LE $\lambda_0 \equiv -1$. The consistency correlation is $\gamma^2 = 1$ for all parameter values if we neglect noise effects, and like other typical delay systems it shows a delay echo with $\alpha \neq 0$. For large feedbacks $|\kappa| \gg 1$, however, this delay echo vanishes. Thus, the laser with optical feedback, and the Ikeda system which models an electro-optic oscillator, are very distinct in terms of the relationships between the characteristic correlation measures. This relates to qualitatively different forms of transformation of the delayed feedback signal. A high value of the transformation correlation α close to its consistency limit indicates, that the signal transformation can be regarded as mostly linear apart from the inconsistent component. If in contrast the spread between α and γ is large, this is because of a high degree of nonlinearity in the consistent part of the transformation. Note that this nonlinear relationship might be too intricate to be detected reliably even by more advanced time series measures [15,16,34,44].

The most direct way to study the effect of consistency in the correlation echoes, and to compare the experimental results with the theory, is to locate the experimental correlation values relative to the theoretical boundaries according to Eq. (15). The precondition of the theory is a complete symmetry between original and replica. It is therefore interesting to ask whether the inevitable experimental parameter mismatches will result in violation of the predictions or whether the elliptic domain is robust against typical small perturbations. Noise occurring in experiment is principally incorporated in the theory. Measurement noise can be regarded as a direct contribution to the inconsistent response component, unless it is desired to quantify the dynamical properties of the system only.

From the experimental time series we select an example for low and high consistency values. For each condition, we obtain the α and β values from the auto-correlation functions of original and replica time series. A predefined window $\Delta t \in [t_1, t_2]$ around the delay time is selected, in which the delay echoes are significantly above the noise floor. The delay time τ is the short-loop roundtrip time. It is worth mentioning that we could have also obtained similar delay echoes from the cross-correlation function. However, with the finite sampling the central consistency correlation peak position does not automatically coincide with sampling points. Moreover, mismatches between original and replica affect the cross-correlation echoes stronger than the autocorrelation echoes. In Fig. 12, the echoes $\alpha(\Delta t)$ and $\beta(\Delta t)$ are plotted against each other within the corresponding consistency ellipse Eq. (15).

It is evident that for the selected conditions the theoretical boundaries are not violated. While this does not imply any general statement on the robustness with respect to mismatches, we can at least exclude a strong sensitivity to small perturbations of the scheme. The peak signatures individually show some oscillations which, however, are almost in phase for α and β, so that their portrait practically collapses onto a single line. The line is located between the identity line $\beta = \alpha$ and the "neutral" line $\beta = \alpha\gamma^2$. The latter is interpreted such that the transformation of the signal from input to output does not distinguish between consistent and inconsistent component. If we assume that this neutrality is a typical condition for the laser system, the deviation toward the identity line can be regarded as a result of measurement noise. In other words,

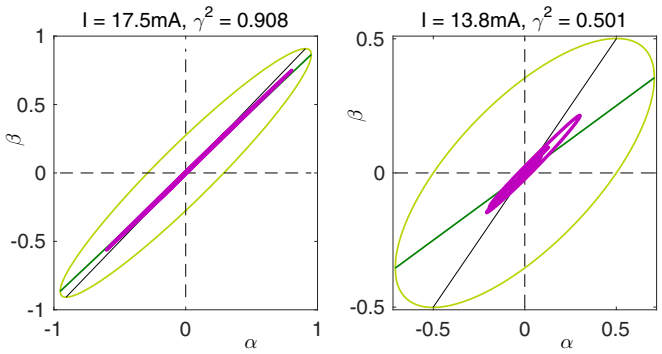

FIG. 12. Examples of AC delay echoes (thick violet) within the corresponding analytic consistency ellipse Eq. (15) (light green). The first delay echo around the main delay time τ is calculated for the original signal yielding the α values, and from the replica signal yielding the corresponding β values. Left panel: high consistency example. Right panel: low consistency example. Note the different scales. The peak structures tend to collapse approximately on a single line between identical ($\alpha = \beta$, black) and neutral line ($\beta = \alpha\gamma^2$, dark green). Delay echoes from other conditions (not shown) have a similar appearance. Despite experimental conditions, the boundaries of the ellipse are never violated.

the experimental peaks might indicate the noise-free neutral line of an ellipse with higher consistency than the plotted one which corresponds to the measured consistency correlation. Numerical simulations of similar systems might in the future provide more insight into this feature.

D. Beyond the ellipse

The experimental correlation functions reveal more than what is covered by the analytical relationships behind the ellipse. In Fig. 10, there are two particular findings worth mentioning. First, the peak structure of the AC functions from original and replica around zero time shift coincides very well. In view of the deviations between the first delay echoes captured by α and β, this result is surprising. Note, however, that this deviation between α and β stems from the input-output relationship that is revealed in the vicinity of the delay time. For time shifts significantly smaller than the delay, the oscillation patterns of original and replica are not distinguishable [39], which is reflected in the central peak structure.

Second, the consistency correlation is picked up only at zero time shift. The central peak structure enclosing this particular point gives us further insight into the relationship between original and replica. The peak structure appears symmetric within the experimental accuracy. This is supported by an analytical argument. Since the CC of the inconsistent components is zero, the remaining contribution to the CC stems from the consistent component which is identical for original and replica. Hence, the CC zero peak is proportional to the self-projection of the consistent component and therefore symmetric; see also Fig. 7. We further observe that the peak is largely proportional to the central AC structure that we discussed before. This, however, lacks a rigorous argument and is a specific property of the laser dynamics. It means that the ratio of the contributions of consistent component and inconsistent component to the zero peak remains constant for the considered interval of time shifts. It might be related to the neutrality hypothesis that we discussed before for the relationship of the α and β peaks. Further investigations including different feedback systems could shed more light on this property.

V. CONCLUSION

We have studied basic relationships between correlation coefficients in a replica scheme in closed-loop and open-loop configuration. In this scheme, we considered stationary time series from a generic delay system with large delays exhibiting chaotic dynamics. We focused on three distinctive coefficients: α, the input-output correlation characterizing the transformation of signals by the nonlinear nodes; β, the spurious correlation resulting only from the correlation α in the drive of the node; and γ^2, the consistency correlation measuring the degree of reliability of the node to repeated identical inputs. We found that, for a given value of the consistency, the other two correlation coefficients are bounded to an elliptic domain whose size is monotonically increasing with γ. The analytical derivation of the ellipse already reveals an interpretation of this dependency. The response of a nonlinear node to its input is split into a completely consistent component and a completely inconsistent component. By numerical results of the logistic map with delayed feedback, we confirmed the analytical calculations and illustrated the decomposition into the two components. Moreover, we identified the value of γ, the root of the consistency correlation, as the inherent consistency which defines the fundamental limit of inferring the output of a driven system from its input only.

We have also verified our consistency theory in a semiconductor laser setup, in which optical delayed feedback gives rise to broadband chaotic dynamics. A double-delay-loop experiment realizes the replica scheme to determine the consistency of the laser with respect to its feedback drive. The laser is driven repeatedly by the chaotic signals generated in a short loop, and by the replay of these signals that have been stored in a long loop. We have analyzed the correlation signatures from the experimental intensity time series. The transformation correlation α is the autocorrelation around the primary delay time. The spurious correlation β is the same autocorrelation signature but in the time series of the replay from the secondary delay line. The consistency correlation γ^2 is the correlation between original and replica without time shift. All experimental signatures are in excellent agreement with the theory.

Our results contribute towards an unraveling of the question: In which way, and to which extent, is the signal transformation by a nonlinear dynamical system related to chaotic variability? This problem appears in the context of driven dynamical systems in general and neuro-inspired information processing in particular, where generic nonlinear systems are employed instead of neural oscillators or simple activation functions. We suggest that our approach based on the replica setup is the most reliable way to access the consistency property. The perspective of two distinct components in the input-output transformation does not only open alternative pathways to the study of delay systems. Together with the resulting consistency limit, it is relevant for the general case of a driven system, in

which input and output have different properties, including nonstationarity.

ACKNOWLEDGMENTS

This work was supported by MINECO (Spain), through projects IDEA No. TEC2016-80063-C3 (AEI/FEDER, UE) and Triphop No. TEC2012-36335 (AEI/FEDER, UE), Comunitat Autònoma de les Illes Balears and FEDER under Grups Competitius. N.O. was funded by a JAE-PreDoc grant from CSIC. T.J. acknowledges support by a fellowship within the Postdoc-Programme of the German Academic Exchange Service (DAAD). The work of M.C.S. has been supported by MINECO (Spain) through a Ramon y Cajal Fellowship (Grant No. RYC-2015-18140).

APPENDIX: PROPERTIES OF THE (IN-)CONSISTENT RESPONSE COMPONENT

1. Definition of the consistent component

Given the responses $x(t)$ and $y(t)$ of two identical units driven by the same signal $x(t-\tau)$, the consistency correlation reads $\gamma^2 = \langle x(t)y(t)\rangle$, given the typical normalization. We now extend the setup to an ensemble of J identical units like in Sec. III B for the logistic maps, with the responses $y_1(t), y_2(t), \ldots, y_J(t)$. Each of these time series is representative in the sense that the correlation of any pair of two responses reveals γ^2. Hence, we rewrite the consistency correlation as an intercorrelation of the ensemble:

$$\gamma^2 = \frac{2}{J(J-1)} \sum_{i<j}^{J} \langle y_i(t) y_j(t)\rangle_t .$$

In the limit of $J \to \infty$ this term becomes the product of the ensemble means $\gamma^2 = \langle f(t)^2\rangle_t$ with $f(t) = \langle y_i(t)\rangle_i$. We denote this ensemble mean $f(t)$ as the consistent component of the response with respect to the correlation measure, because the consistency correlation is directly determined by this mean. One may conclude that a different measure for consistency would result in another decomposition of an individual response signal into consistent and inconsistent component.

2. Correlation between consistent and inconsistent component

We consider a single input-output transformation, in which we produce an ensemble of equivalent output realizations simultaneously. Let $x_i(t)$ be such a single output, with i being the ensemble index. We assume the time series to be stationary and with ergodicity properties that we will explicitly use in the following calculations. With respect to the linear correlation functions, we average over the ensemble to obtain the time-dependent mean, which we denote as the consistent component of the response, or the consistent part of the transformation,

$$f(t) = \langle x_i(t)\rangle_i .$$

The difference to this mean is the inconsistent component of the response

$$n_i(t) = x_i(t) - f(t).$$

Our goal is to show that, by this definition, the correlation between consistent and inconsistent component vanishes for all time shifts Δ, i.e., for $t' = t + \Delta$, $\langle f(t) n_i(t')\rangle_t = 0$. First, from the definition follows directly that the ensemble mean of $n_i(t)$ vanishes for all times

$$\langle n_i(t)\rangle_i = 0.$$

This property of the ensemble distribution function of $n_i(t)$ affects distribution functions obtained by the single realization over time. Let t_k, $k \in \mathbb{N}$ be the times at which the consistent response takes a certain value, $f(t_k) = \phi$. The distribution obtained from all the values $n_i(t_k)$ is $\rho(n|\phi)$, and since every $n_i(t_k)$ is drawn from a distribution with zero mean, the mean of ρ must be zero as well according to the central limit theorem

$$\int n\rho(n|\phi)dn = 0.$$

The same argument holds for different conditioning of the distribution to time-shifted arguments or to more than a single sample of f. We apply this property to calculate the correlation function

$$\begin{aligned}\langle f(t) n_i(t')\rangle_t &= \int df_t \int dn_{t'}\, f_t n_{t'} \rho(f_t, n_{t'}) \\ &= \int df_t f_t \rho_f(f_t) \int dn_{t'} n_{t'} \rho_n(n_{t'}|f_t) \\ &= 0. \end{aligned} \tag{A1}$$

We can also apply this procedure to correlations between different realizations $n_i(t)$ and $n_j(t')$ of the inconsistent component. The time average is the same for all $i \neq j$, and the realizations are drawn independently from their distribution at each time, so that for $t' = t + \Delta$,

$$\langle n_i(t) n_j(t')\rangle_t = 0. \tag{A2}$$

The vanishing numerical correlation functions from the ensemble of driven logistic maps in Fig. 7 clearly illustrate these results.

[1] S. Boccaletti, J. Kurths, G. Osipov, D. Valladares, and C. Zhou, Phys. Rep. **366**, 1 (2002).

[2] A. Arenas, A. Díaz-Guilera, J. Kurths, Y. Moreno, and C. Zhou, Phys. Rep. **469**, 93 (2008).

[3] N. F. Rulkov, M. M. Sushchik, L. S. Tsimring, and H. D. I. Abarbanel, Phys. Rev. E **51**, 980 (1995).

[4] L. Kocarev and U. Parlitz, Phys. Rev. Lett. **76**, 1816 (1996).

[5] O. I. Moskalenko, A. A. Koronovskii, A. E. Hramov, and S. Boccaletti, Phys. Rev. E **86**, 036216 (2012).

[6] O. I. Moskalenko, A. A. Koronovskii, and A. E. Hramov, Phys. Rev. E **87**, 064901 (2013).

[7] W. Maass, T. Natschläger, and H. Markram, Neural Comput. **14**, 2531 (2002).

[8] H. Jaeger and H. Haas, Science **304**, 78 (2004).

[9] D. Brunner, M. C. Soriano, C. R. Mirasso, and I. Fischer, Nat. Commun. **4**, 1364 (2013).
[10] M. Hermans, M. Burm, T. Van Vaerenbergh, J. Dambre, and P. Bienstman, Nat. Commun. **6**, 6729 (2015).
[11] R. Albert and A.-L. Barabási, Rev. Mod. Phys. **74**, 47 (2002).
[12] J. F. Donges, Y. Zou, N. Marwan, and J. Kurths, Eur. Phys. J. Special Topics **174**, 157 (2009).
[13] G. Giacomelli, S. Barland, M. Giudici, and A. Politi, Phys. Rev. Lett. **104**, 194101 (2010).
[14] P. T. Clemson and A. Stefanovska, Phys. Rep. **542**, 297 (2014).
[15] J. Schumacher, R. Haslinger, and G. Pipa, Phys. Rev. E **85**, 056215 (2012).
[16] U. Parlitz, Nonlin. Theory Appl. **3**, 113 (2012).
[17] L. M. Pecora and T. L. Carroll, Phys. Rev. Lett. **64**, 821 (1990).
[18] K. Pyragas, Phys. Rev. E **56**, 5183 (1997).
[19] A. Uchida, K. Yoshimura, P. Davis, S. Yoshimori, and R. Roy, Phys. Rev. E **78**, 036203 (2008).
[20] T. Jüngling, M. C. Soriano, and I. Fischer, Phys. Rev. E **91**, 062908 (2015).
[21] A. Uchida, R. McAllister, and R. Roy, Phys. Rev. Lett. **93**, 244102 (2004).
[22] K. Kanno and A. Uchida, Phys. Rev. E **86**, 066202 (2012).
[23] N. Oliver, T. Jüngling, and I. Fischer, Phys. Rev. Lett. **114**, 123902 (2015).
[24] N. Oliver, L. Larger, and I. Fischer, Chaos **26**, 103115 (2016).
[25] J. Nakayama, K. Kanno, and A. Uchida, Opt. Express **24**, 8679 (2016).
[26] J. Bueno, D. Brunner, M. C. Soriano, and I. Fischer, Opt. Express **25**, 2401 (2017).
[27] S. Heiligenthal, T. Jüngling, O. D'Huys, D. A. Arroyo-Almanza, M. C. Soriano, I. Fischer, I. Kanter, and W. Kinzel, Phys. Rev. E **88**, 012902 (2013).
[28] X. Porte, M. C. Soriano, and I. Fischer, Phys. Rev. A **89**, 023822 (2014).
[29] H. D. I. Abarbanel, N. F. Rulkov, and M. M. Sushchik, Phys. Rev. E **53**, 4528 (1996).
[30] A. Kittel, J. Parisi, and K. Pyragas, Physica D (Amsterdam) **112**, 459 (1998).
[31] A. Uchida, R. McAllister, R. Meucci, and R. Roy, Phys. Rev. Lett. **91**, 174101 (2003).
[32] W. He and J. Cao, Chaos **19**, 013118 (2009).
[33] S. Heiligenthal, T. Dahms, S. Yanchuk, T. Jüngling, V. Flunkert, I. Kanter, E. Schöll, and W. Kinzel, Phys. Rev. Lett. **107**, 234102 (2011).
[34] M. C. Soriano, G. Van der Sande, I. Fischer, and C. R. Mirasso, Phys. Rev. Lett. **108**, 134101 (2012).
[35] R. Vicente, T. Pérez, and C. R. Mirasso, IEEE J. Quantum Electron. **38**, 1197 (2002).
[36] G. Van der Sande, M. C. Soriano, I. Fischer, and C. R. Mirasso, Phys. Rev. E **77**, 055202(R) (2008).
[37] F. T. Arecchi, G. Giacomelli, A. Lapucci, and R. Meucci, Phys. Rev. A **45**, R4225 (1992).
[38] X. Porte, O. D'Huys, T. Jüngling, D. Brunner, M. C. Soriano, and I. Fischer, Phys. Rev. E **90**, 052911 (2014).
[39] M. C. Soriano, V. Flunkert, and I. Fischer, Chaos **23**, 043133 (2013).
[40] G. Giacomelli, R. Meucci, A. Politi, and F. T. Arecchi, Phys. Rev. Lett. **73**, 1099 (1994).
[41] S. Yanchuk and G. Giacomelli, J. Phys. A **50**, 103001 (2017).
[42] F. M. Atay, J. Jost, and A. Wende, Phys. Rev. Lett. **92**, 144101 (2004).
[43] M. C. Soriano, J. García-Ojalvo, C. R. Mirasso, and I. Fischer, Rev. Mod. Phys. **85**, 421 (2013).
[44] H. Kato, M. C. Soriano, E. Pereda, I. Fischer, and C. R. Mirasso, Phys. Rev. E **88**, 062924 (2013).